

Influence of intrinsic decoherence on entanglement teleportation via a Heisenberg XYZ model with different Dzyaloshinskii–Moriya interactions

Meng Qin^{1,2} · Zhong-Zhou Ren^{1,3,4}

Received: 18 November 2014 / Accepted: 18 March 2015 / Published online: 2 April 2015
© Springer Science+Business Media New York 2015

Abstract We investigate the characteristics of entanglement teleportation of a two-qubit and three-qubit Heisenberg XYZ model under different Dzyaloshinskii–Moriya (DM) interactions with intrinsic decoherence taken into account. The two-qubit results reveal that the dynamics of entanglement is a symmetric function about the coupling coefficient J for the z -component DM system, whereas it is not for the x -component DM system. The ferromagnetic case is superior to the antiferromagnetic case to restrain decoherence when using the x -component DM system. The dependencies of entanglement, the output entanglement, and the average fidelity on initial state angle α all demonstrate periodicity. Moreover, the x -component DM system can get a high fidelity both in two-qubit and in three-qubit teleportation protocol.

Keywords Entanglement · Decoherence · Teleportation · Different Dzyaloshinskii–Moriya interactions

1 Introduction

Quantum entanglement is the fundamental characteristic of quantum mechanics, and it is also an important resource for quantum communication and quantum computa-

✉ Meng Qin
qrainm@gmail.com

¹ Department of Physics and Key Laboratory of Modern Acoustic, Nanjing University, Hankou Road 22, Nanjing 210093, China

² College of Sciences, PLA University of Science and Technology, Nanjing 211101, China

³ Center of Theoretical Nuclear Physics, National Laboratory of Heavy-Ion Accelerator, Lanzhou 730000, China

⁴ Kavli Institute for Theoretical Physics, Chinese Academy of Sciences, Beijing 100190, China

tion [1]. Recently, much attention has been paid to the thermal entanglement in the spin model [2,3] since it plays a key role in quantum information processing tasks. The experimental observation of thermal entanglement in a spin chain formed in the compound $\text{Na}_2\text{Cu}_5\text{Si}_4\text{O}_{14}$ has been reported [4]. In particular, the properties of Heisenberg model with the Dzyaloshinskii–Moriya (DM) interaction (arising from spin–orbit coupling) have been studied extensively which can cause another type of anisotropy [5–8]. The Cs_2CuCl_4 , Cu benzoate, and kagomé antiferromagnet can be described by the DM interaction. Many physical systems, such as optical lattices, superconductors, and nuclear spins also have been simulated by the model. It is now well established that at low temperatures these systems exhibit new types of magnetic order and novel quantum phases [9]. Moreover, quantum teleportation has been comprehensively studied in both theoretical and experimental works. Quantum teleportation can be adopted to test the existence of entanglement and how much entanglement there is in a quantum state. Quantum teleportation not only is relevant to quantum communication, but also is a universal computational primitive for quantum computation. It is worthwhile to study the entanglement teleportation in the condensed matter physics.

Recently, Li et al. [8] examined the Heisenberg model with different DM interactions. They found that a more efficient control parameter can be obtained by adjusting the direction of the DM interaction, no matter in the antiferromagnetic case or in the ferromagnetic case. Inspired by this, if we use the Heisenberg model with different DM interactions to perform quantum teleportation protocol, we will also have another means to manipulate the output entanglement and the fidelity of entanglement teleportation. As far as we are aware, the entanglement in the system must be maintained a long time in order to fulfill the quantum task. The unavoidable interaction of a system with its surroundings always makes entanglement decay with time [10]. It is difficult to keep the coherence of a quantum state as the quantum system correlates with its external environment. So, all the discussion must be including the environmental effect on the system [10,11]. In recent years, there have been many proposals to solve the decoherence problem which is responsible for the quantum-to-classical transition. The general investigation method for this problem is tracing out all other degrees except the quantum states of interest. However, Milburn [12] has given a simple model of intrinsic decoherence based on the assumption that for sufficiently short time steps the system does not evolve continuously under unitary evolution but rather in a stochastic sequence of identical unitary transformations [13–15]. The effects of intrinsic decoherence on the dynamics of entanglement have been studied in a number of works. For example, Hu [15] has shown that the ideal spin channels will be destroyed by the intrinsic decoherence environment. Yu [16] has discussed the intrinsic decoherence effects on the entanglement of a two-qubit XYZ model. Also, the results of reference [17] has demonstrated that an inhomogeneous magnetic field can reduce the effects of intrinsic decoherence. Fan has found that the phase decoherence rate makes the original harmonic vibration with respect to time decay to a stable value [18]. All those works enrich our understanding of the decoherence mechanism. However, how the different DM interactions affect the dynamics of entanglement teleportation and the fidelity of entanglement teleportation has not been reported. We will not only study how much entanglement is teleported through the channel, but also consider the quality of the entanglement teleportation protocol by the fidelity.

In this paper, we will investigate the influence of the intrinsic decoherence on the entanglement and entanglement teleportation of a two-qubit and three-qubit Heisenberg XYZ model with different DM interactions. The outline of this work is as follows. In Sect. 2, we introduce the Hamiltonian of the two-qubit model with different DM interactions and present the exact solution of the model. In Sect. 3, we discuss the effect of different DM interactions on the evolution of entanglement. In Sect. 4, entanglement teleportation processes via the above system and the effect of initial state on the fidelity are investigated. In Sect. 5, we extend our result to three-qubit DM system and study the effect of decoherence on the average fidelity. Finally, in Sect. 6, we summarize our results and draw our conclusions.

2 Model and solution

The Hamiltonian H_z for a two-qubit anisotropic Heisenberg XYZ model with z -component DM interaction is

$$H_z = J(1 + \gamma)\sigma_1^x\sigma_2^x + J(1 - \gamma)\sigma_1^y\sigma_2^y + J_z\sigma_1^z\sigma_2^z + D_z(\sigma_1^x\sigma_2^y - \sigma_1^y\sigma_2^x), \quad (1)$$

where J is the isotropic coupling coefficient and J_z is the anisotropic coupling coefficient. They both can be obtained by combining bare exchange interactions with an applied field [19]. $J > 0$ and $J_z > 0$ correspond to the antiferromagnetic. $J < 0$ and $J_z < 0$ correspond to the ferromagnetic. γ is the anisotropic parameter. D_z is the z -component DM interaction parameter, and $\sigma^i (i = x, y, z)$ are Pauli matrices. The eigenvalues and eigenvectors of the Hamiltonian H_z are given by

$$\begin{aligned} E_{z1} &= J_z + 2J\gamma, \\ E_{z2} &= J_z - 2J\gamma, \\ E_{z3} &= -J_z + 2\sqrt{J^2 + D_z^2}, \\ E_{z4} &= -J_z - 2\sqrt{J^2 + D_z^2}, \\ |\psi_{z1,z2}\rangle &= \frac{|00\rangle \pm |11\rangle}{\sqrt{2}}, \\ |\psi_{z3,z4}\rangle &= \frac{|01\rangle \pm \chi|10\rangle}{\sqrt{2}}, \end{aligned} \quad (2)$$

where $\chi = \frac{J - iD_z}{\sqrt{J^2 + D_z^2}}$.

The Hamiltonian H_x for a two-qubit anisotropic Heisenberg XYZ model with x -component DM interaction is

$$H_x = J(1 + \gamma)\sigma_1^x\sigma_2^x + J(1 - \gamma)\sigma_1^y\sigma_2^y + J_z\sigma_1^z\sigma_2^z + D_x(\sigma_1^y\sigma_2^z - \sigma_1^z\sigma_2^y). \quad (3)$$

Except for D_x , the meanings of the other parameters are the same as those in Eq. (1). The eigenvalues and eigenvectors of the Hamiltonian H_x are given by

$$\begin{aligned}
 E_{x1} &= 2J - J_z, \\
 E_{x2} &= 2J\gamma + J_z, \\
 E_{x3} &= -J(1 + \gamma) + \sqrt{[J(1 - \gamma) + J_z]^2 + 4D_x^2}, \\
 E_{x4} &= -J(1 + \gamma) - \sqrt{[J(1 - \gamma) + J_z]^2 + 4D_x^2}, \\
 |\psi_{x1}\rangle &= \frac{|01\rangle + |10\rangle}{\sqrt{2}}, \\
 |\psi_{x2}\rangle &= \frac{|00\rangle + |11\rangle}{\sqrt{2}}, \\
 |\psi_{x3}\rangle &= \frac{\sin\varphi_1|00\rangle - i\cos\varphi_1|01\rangle + i\cos\varphi_1|10\rangle - \sin\varphi_1|11\rangle}{\sqrt{2}}, \\
 |\psi_{x4}\rangle &= \frac{\sin\varphi_2|00\rangle + i\cos\varphi_2|01\rangle - i\cos\varphi_2|10\rangle - \sin\varphi_2|11\rangle}{\sqrt{2}}, \quad (4)
 \end{aligned}$$

here $\varphi_{1,2} = \arctan\left(\frac{2D_x}{\sqrt{[J(1-\gamma)+J_z]^2+4D_x^2} \mp J(1-\gamma) \pm J_z}\right)$.

The master equation describing the intrinsic decoherence under the Markovian approximations is given by [12, 14]

$$\frac{d\rho(t)}{dt} = -i[H, \rho(t)] - \frac{1}{2}\Gamma[H, [H, \rho(t)]], \quad (5)$$

where Γ is the intrinsic decoherence rate. The formal solution of the above master equation can be expressed as

$$\rho(t) = \sum_{k=0}^{\infty} \frac{(t)^k}{k!} M^k \rho(0) M^{\dagger k}, \quad (6)$$

where $\rho(0)$ is the density operator of the initial state and M^k is defined by

$$M^k = H^k e^{-iHt} e^{-\frac{1}{2}\Gamma H^2}. \quad (7)$$

According to the Eq. (6), it is easy to show that, under intrinsic decoherence, the dynamics of the density operator $\rho(t)$ for the above-mentioned system which is initially in the state $\rho(0)$ is given by

$$\rho(t) = \sum_{mn} \exp\left[-\frac{\Gamma t}{2}(E_m - E_n)^2 - i(E_m - E_n)t\right] \times \langle\psi_m|\rho(0)|\psi_n\rangle |\psi_m\rangle \langle\psi_n|, \quad (8)$$

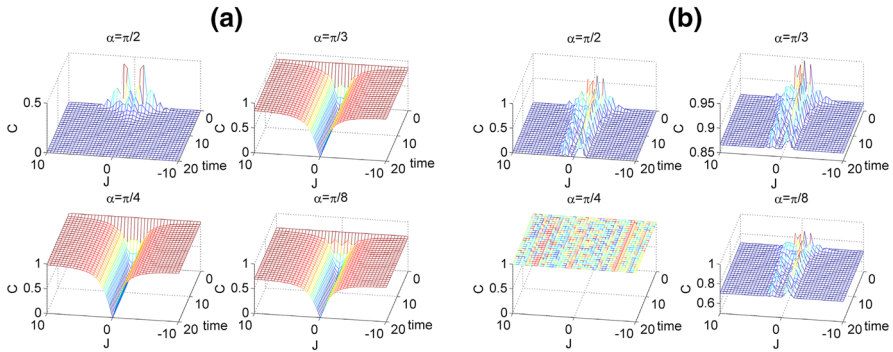


Fig. 1 Concurrence versus the real coupling coefficients J and the time under different initial states with the Hamiltonian being Eq. (1) (a), Eq. (3) (b). $\gamma = 0.2, J_z = 1, D_{z/x} = 2, \Gamma = 0.02$.

where E_m, E_n and $|\psi_m\rangle, |\psi_n\rangle$ are the eigenvalues and the corresponding eigenvectors of $H_{z/x}$ given in Eqs. (2) and (4). Here, we will choose $|\varphi(0)\rangle = \cos \alpha |01\rangle + \sin \alpha |10\rangle$ as the initial state for two-qubit Heisenberg XYZ model.

3 Entanglement evolutions

To quantify the amount of entanglement associated with $\rho(t)$, we consider the concurrence, which is defined as [20,21]

$$C = \max \left[0, 2\max(\lambda_i) - \sum_i^4 \lambda_i \right], \tag{9}$$

where λ_i are the square roots of the eigenvalues of the matrix $R = \rho(t)S\rho^*(t)S$, $\rho(t)$ is the density matrix, $S = \sigma_1^y \otimes \sigma_2^y$, and the asterisk stands for the complex conjugate.

In Fig. 1, we depict the concurrence as a function of the coupling coefficients J and the time under different initial conditions. As is shown in Fig. 1a, there is no difference between ferromagnetic case and antiferromagnetic case because the concurrence is a symmetric function about $J = 0$. This can be explained from Eq. (2), for the eigenvalues are the same if we change the sign of J . The concurrence is a decreasing function with respect to $|J|$ when the initial state is a separable state, and it is an increasing function for the entangled state. In Fig. 1b, we see that the concurrence is an asymmetric function with the $J = 0$ for the D_x system because the eigenvalues will change if we alter the sign of J . So the evolution of entanglement is different for the antiferromagnetic case and the ferromagnetic case. When the initial state angle become $\alpha = \pi/4$, the entanglement is 1 and it is independent of any parameters.

In Fig. 2, the entanglement is plotted versus the coupling coefficients J_z and the time. From Fig. 2a, we see that the entanglement is also a symmetric function about $J_z = 0$ because the expression of the density matrix for this system is independent of J_z . After enough time of decoherence, the entanglement becomes a constant value,

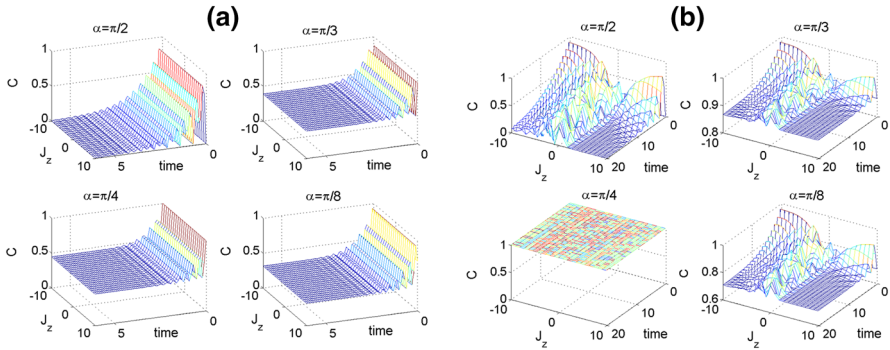


Fig. 2 Concurrence versus the real coupling coefficients J_z and the time under different initial states with the Hamiltonian being Eq. (1) (a), Eq. (3) (b). $J = 1, \gamma = 0.5, D_{z/x} = 2, \Gamma = 0.02$

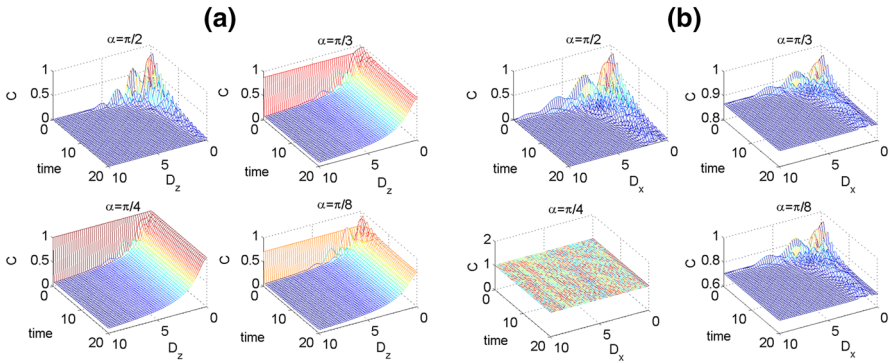


Fig. 3 Concurrence versus the DM interaction $D_{z/x}$ and the time under different initial states with the Hamiltonian being Eq. (1) (a), Eq. (3) (b). $J = 1, \gamma = 0.6, J_z = 1.5, \Gamma = 0.02$

while the system becomes a stable state when $\text{time} \rightarrow \infty$. In Fig. 2b, the entanglement is an asymmetric function with respect to $J_z = 0$ except for $\alpha = \pi/4$ (the entanglement assumes its maximum 1 under this condition). We can note that with the increase in time the entanglement behaves as an oscillatory function, especially for ferromagnetic case.

In Fig. 3, we give the plot of the entanglement as a function of the DM interaction $D_{z/x}$ and the time. Except the initial state $|10\rangle$, the other figures in Fig. 3a show that the entanglement is a monotonic decreasing function with respect to D_z . For a fixed D_z , the entanglement will quickly become a stable value with the increase in time because the stable decoherence time is short for this condition. In Fig. 3b, except $\alpha = \pi/4$ case, the entanglement will oscillate with the increase in D_x and eventually become a stable value. This result can be explained by seeking the limiting value of the concurrence equation.

Fig. 4 gives the results about how the initial state affects the entanglement. In Fig. 4a, with the increasing of the time, the entanglement will quickly become a stable value. The maximal stable value of concurrence occurs at $\alpha = \pi/4$ and $\alpha = 3\pi/4$.

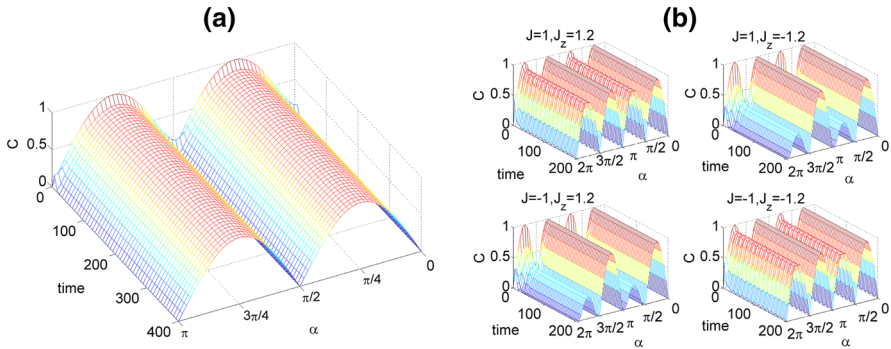


Fig. 4 Concurrence versus the initial state angle α and the time with the Hamiltonian being Eq. (1) a, Eq. (3) (b). **a** $J = 1, \gamma = 0.2, J_z = 2, D_z = 0.5, \Gamma = 0.02$. **b** $\gamma = 0.2, D_x = 0.5, \Gamma = 0.02$

The dependence of entanglement on initial state angle α periodically changes, and the period is $\pi/2$. In Fig. 4b, we find that the region of the entanglement will change if we alter the sign for J or J_z , but the results will not be affected if their signs change together. The period is $\pi/2$ for the same signs of J and J_z , but the period is π for different signs of J and J_z .

4 The effect of initial state on the entanglement teleportation and the fidelity

The above model can be used as a quantum channel to transmit unknown state. After we input a state from one end, the state will be destroyed, and then, we can apply a local measurement in the form of linear operators, after that we will get the output state from another end. Now we use two copies of the above state $\rho(t) \otimes \rho(t')$ as resource and input state $|\psi_{in}\rangle = \cos(\theta/2)|10\rangle + e^{i\phi} \sin(\theta/2)|01\rangle$ ($0 \leq \theta \leq \pi, 0 \leq \phi \leq 2\pi$). The output replica state can be obtained by $\rho_{out}(t) = \sum_{i,j} p_{ij}(\sigma_i \otimes \sigma_j)\rho_{in}(\sigma_i \otimes \sigma_j)$ [22], where σ_i ($i = 0, x, y, z$) denote the unit matrix I and three components of the Pauli matrix, respectively, $\rho_{in} = |\psi\rangle_{in} \langle\psi|$ and $p_{ij} = tr [E^i \rho(t)] tr [E^j \rho(t)], \sum p_{ij} = 1$. $\rho(t)$ is the quantum state of the channel, $E^0 = |\psi_{Bell}^2\rangle \langle\psi_{Bell}^2|, E^1 = |\psi_{Bell}^3\rangle \langle\psi_{Bell}^3|, E^2 = |\psi_{Bell}^0\rangle \langle\psi_{Bell}^0|, E^3 = |\psi_{Bell}^1\rangle \langle\psi_{Bell}^1|$ and $|\psi_{Bell}^{0,3}\rangle = (|00\rangle \pm |11\rangle)/\sqrt{2}, |\psi_{Bell}^{1,2}\rangle = (|01\rangle \pm |10\rangle)/\sqrt{2}$.

In Fig. 5, the output entanglement C_{out} as a function of the initial state angle α and the time is plotted for the $D_{z/x}$ system. From the figures, we find that the maximal output entanglement is decreasing when the input state angle θ varied from $\pi/2$ to $\pi/6$. The periodic dependence of output entanglement on the angle α also exists in the figures. $\pi/2$ and π are the periodicity for the D_z system and the D_x system, respectively. Moreover, in Fig. 5b, the behavior of the output entanglement is totally different when the initial state angle $\alpha \in (0, \pi/2)$ and $\alpha \in (\pi/2, \pi)$. These results demonstrate that how to choose initial state is very important.

The fidelity between ρ_{in} and ρ_{out} characterizes the quality of the teleported state ρ_{out} . When the input is a pure state, we can apply the concept of fidelity as a useful

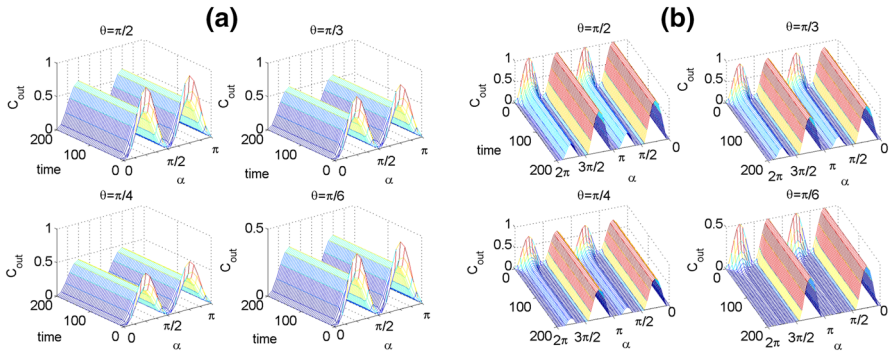


Fig. 5 Entanglement of output state versus the initial state angle α and the time t with the Hamiltonian being Eq. (1) (a), Eq. (3) (b). $J = 1, \gamma = 0.2, D_{z/x} = 0.5, \phi = 0, \Gamma = 0.02$, (a), (b)

indicator of teleportation performance of a quantum channel. If the quantum channel is maximal entangled, the best entanglement teleportation will be obtained. The fidelity of ρ_{in} and ρ_{out} is defined to be [23,24]

$$F(\rho_{in}, \rho_{out}) = \{tr[\sqrt{(\rho_{in})^{1/2}\rho_{out}(\rho_{in})^{1/2}}]\}^2. \tag{10}$$

By averaging over all possible input state, the average fidelity F_A of teleportation can be formulated as

$$F_A = \frac{\int_0^{2\pi} d\phi \int_0^\pi F \sin \theta d\theta}{4\pi}. \tag{11}$$

In Fig. 6, the average fidelity F_A is plotted as a function of the time under different initial state α . For the purpose of transmitting ρ_{in} with better fidelity than any classical communication protocol, we require Eq. (11) to be strictly greater than $2/3$ [25]. Figure 6a gives the evolution of fidelity for the $D_{z/x}$ system when the initial state is $|10\rangle$. In this figure, the D_x system behaves inferior to the classical communication and the D_z system performs better. If we change the initial state from $|10\rangle$ to $(\sqrt{3}|10\rangle + |01\rangle)/2$, the result in Fig. 6b shows that the two kinds of system all behave better than the former condition. The entanglement will become a stable constant value with the increase in time, and this is meaningful for quantum information processing. In Fig. 6c, d, we choose the initial state as $\sqrt{2}(|10\rangle + |01\rangle)/2$ and $|\varphi(0)\rangle = 0.9238|01\rangle + 0.3826|10\rangle$, respectively, the D_x system has a better average fidelity than the D_z system. From Fig. 6, we find that the initial state is one of the significant factors to determine what kinds of system are suitable as quantum channel.

The asymptotic behavior of the fidelity versus the model parameters α is shown in the Fig. 7. The asymptotic fidelity F_A demonstrates periodicity too. This means that we can implement teleportation process in proper angle and get optimal fidelity. We note that the period is $\pi/2, \pi$ for the D_z and the D_x systems, respectively.

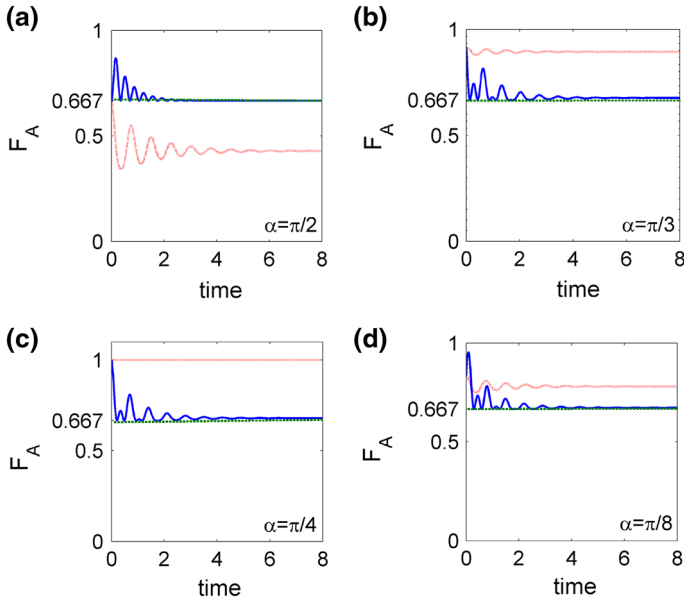


Fig. 6 Dynamics of the average fidelity for $D_z = 2$ (blue solid line) and $D_x = 2$ (red dotted line). $J = 1, \gamma = 0.4, J_z = 0.5, \Gamma = 0.02$ (Color figure online)

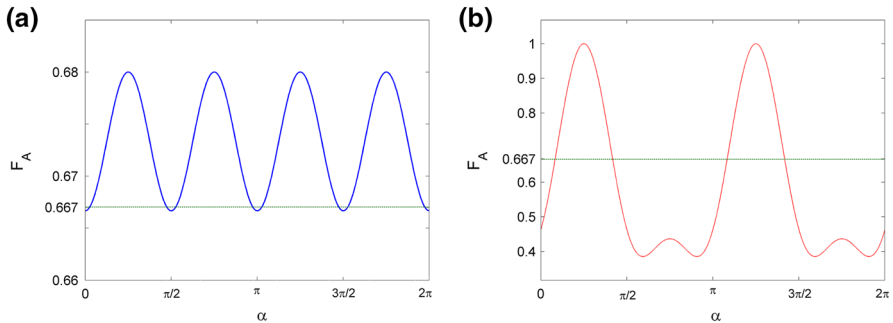


Fig. 7 Asymptotical behavior of the fidelity versus the initial state angle $\alpha. J = 1, \gamma = 0.8, J_z = 2, \Gamma = 0.02$. **a** $D_z = 2$, **b** $D_x = 2$

5 The decoherence of the fidelity for the three-qubit model

The three-qubit Hamiltonian of XYZ model with different DM interactions is expressed as follows,

$$H_z = J(1 + \gamma)(\sigma_1^x \sigma_2^x + \sigma_2^x \sigma_3^x) + J(1 - \gamma)(\sigma_1^y \sigma_2^y + \sigma_2^y \sigma_3^y) + J_z(\sigma_1^z \sigma_2^z + \sigma_2^z \sigma_3^z) + D_z(\sigma_1^x \sigma_2^y - \sigma_1^y \sigma_2^x + \sigma_2^x \sigma_3^y - \sigma_2^y \sigma_3^x), \tag{12}$$

$$H_x = J(1 + \gamma)(\sigma_1^x \sigma_2^x + \sigma_2^x \sigma_3^x) + J(1 - \gamma)(\sigma_1^y \sigma_2^y + \sigma_2^y \sigma_3^y) + J_z(\sigma_1^z \sigma_2^z + \sigma_2^z \sigma_3^z) + D_x(\sigma_1^y \sigma_2^z - \sigma_1^z \sigma_2^y + \sigma_2^y \sigma_3^z - \sigma_2^z \sigma_3^y), \tag{13}$$

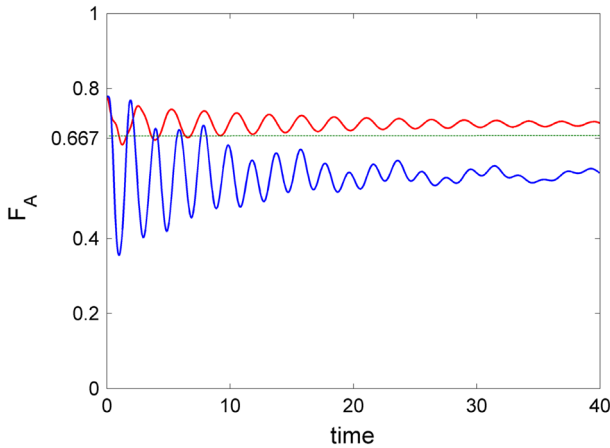


Fig. 8 Dynamics of the average fidelity for $D_z = 1$ (blue solid line) and $D_x = 1$ (red dotted line). The initial state is W state $|W\rangle = (|001\rangle + |010\rangle + |100\rangle)/\sqrt{3}$. $J = 1, \gamma = 0.2, J_z = 1.2, \Gamma = 0.02$ (Color figure online)

Taking into account the decoherence factors, we use the above three-qubit state χ_{ABC} as a quantum resource. The joint state of the two receivers conditioned on the sender measurement result j is described by [26]

$$\rho_{BC}^j = \frac{1}{p_j} tr_{SA} \left[\left(\Pi_{SA}^j \otimes I_{BC} \right) \left(\tau_{in} \otimes \chi_{ABC} \right) \right], \tag{14}$$

here $\Pi_{SA}^1 = |\psi_{Bell}^0\rangle\langle\psi_{Bell}^0|, \Pi_{SA}^2 = |\psi_{Bell}^3\rangle\langle\psi_{Bell}^3|, \Pi_{SA}^3 = |\psi_{Bell}^1\rangle\langle\psi_{Bell}^1|$, and $\Pi_{SA}^4 = |\psi_{Bell}^2\rangle\langle\psi_{Bell}^2|$. I_{BC} is the identity operator on the subsystem BC, and j is the outcome of the measurement. $\tau_{in} = |\psi\rangle_s \langle\psi|$ is the density matrix for input state $|\psi\rangle_s = \cos \frac{\theta}{2} |0\rangle_s + e^{i\phi} \sin \frac{\theta}{2} |1\rangle_s$. $p_j = tr_{SABC} \left[\left(\Pi_{SA}^j \otimes I_{BC} \right) \left(\kappa_s \otimes \chi_{ABC} \right) \right]$. In order to successfully carry out the teleportation protocol, two receivers perform j -dependent unitary operations $U_B^j = U_C^j = U^j$ on the systems B and C, respectively. So

$$\tau_B^j = \tau_C^j = \tau^j = U^j \rho^j U^{j\dagger}, \tag{15}$$

where U^j could be one of the Pauli matrices or the identity matrix. $\rho^j = \rho_B^j = tr_C \rho_{BC}^j = \rho_C^j = tr_B \rho_{BC}^j$. The average fidelity between τ_{in} and τ_{out} characterizes the quality of the teleportation protocol

$$F_A = \frac{\int_0^{2\pi} d\phi \int_0^\pi \sin \theta d\theta \sum_{i=1}^4 p_j tr \left(\tau_{out}^j \tau_{in} \right)}{4\pi}. \tag{16}$$

In Fig. 8, the average fidelity F_A is plotted as a function of the time. The D_x system behaves better than the classical communication, and the D_z system will exhibit

damped oscillation below the value of $2/3$. From this figure and Fig. 6, we notice that the D_x system is more favorable to resist decoherence in most cases.

6 Summary

In summary, we have investigated the entanglement and the fidelity of entanglement teleportation for Heisenberg XYZ model with different Dzyaloshinskii–Moriya interactions when the Milburn’s intrinsic decoherence taken into consideration. After comparing the two different DM interactions, we can clearly find which one can get stable entanglement and high fidelity. The results demonstrate that after reaching the maximum decoherence time the entanglement will keep in a steady value for some initial state. With the change of initial state angle, the entanglement, the output entanglement, and the asymptotic fidelity all will exhibit periodicity. The D_x system is more favorable to resist decoherence and get a high fidelity both in two-qubit teleportation protocol and in three-qubit teleportation protocol. These results are valuable in quantum information processing based on the solid-state qubit.

Acknowledgments This work was supported by the National Natural Science Foundation of China (Grant Nos. 11035001, 11375086, 11105079, and 10975072), the National Major State Basic Research and Development of China (Grant Nos. 2013CB834400 and 2010CB327803), the Chinese Academy of Sciences Knowledge Innovation Project (Grant No. KJCX2-SW-N02), the Research Fund of Doctoral Point (RFDP) (Grant No. 20100091110028), and the Science and Technology Development Fund of Macau (Grant No. 068/2011/A).

References

1. Nielsen, M.A., Chuang, I.L.: Quantum Computation and Quantum Information. Cambridge University Press, Cambridge (2000)
2. Horodecki, R., Horodecki, P., Horodecki, M., Horodecki, K.: Quantum entanglement. *Rev. Mod. Phys.* **81**, 865 (2009)
3. Amico, L., Fazio, R., Osterloh, A., Vedral, V.: Entanglement in many-body system. *Rev. Mod. Phys.* **80**, 517 (2008)
4. Souza, A.M., Reis, M.S., Soares-Pinto, D.O., Oliveira, I.S., Sarthour, R.S.: Experimental determination of thermal entanglement in spin clusters using magnetic susceptibility measurements. *Phys. Rev. B* **77**, 104402 (2008)
5. Qin, M., Li, Y.B., Wu, F.P.: Relations between quantum correlations, purity and teleportation fidelity for the two-qubit Heisenberg XYZ system. *Quantum Inf. Process.* **13**, 1573–1582 (2014)
6. Amniat-Talab, M., Jahromi, H.R.: On the entanglement and engineering phase gates without dynamical phases for a two-qubit system with DM interaction in magnetic field. *Quantum Inf. Process.* **12**, 1185–1199 (2013)
7. Ma, X.S., Zhao, G.X., Zhang, J.Y., Wang, A.M.: Tripartite entanglement of a spin star model with Dzialoshinski–Moriya interaction. *Quantum Inf. Process.* **12**, 321–329 (2013)
8. Li, D.C., Cao, Z.L.: Thermal entanglement in the anisotropic Heisenberg XYZ model with different Dzyaloshinskii–Moriya couplings. *Chin. Phys. Lett.* **26**, 020309 (2009)
9. Majumdar, K.: Magnetic phase diagram of a spatially anisotropic, frustrated spin-1/2 Heisenberg antiferromagnet on a stacked square lattice. *J. Phys.: Condens. Matter* **23**, 046001 (2011)
10. Hu, M.L., Fan, H.: Robustness of quantum correlations against decoherence. *Ann. Phys.* **327**, 851–860 (2012)
11. Man, Z.X., Xia, Y.J.: Quantum teleportation in a dissipative environment. *Quantum Inf. Process.* **11**, 1911–1920 (2012)
12. Milburn, G.J.: Intrinsic decoherence in quantum mechanics. *Phys. Rev. A* **44**, 5401–5406 (1991)

13. Xu, J.B., Zou, X.B., Yu, J.H.: Influence of intrinsic decoherence on nonclassical properties of the two-mode Raman coupled model. *Eur. Phys. J. D* **10**, 295–300 (2000)
14. Mohammadi, H., Akhtarshenas, S.J., Kheirandish, F.: Influence of dephasing on the entanglement teleportation via a two-qubit Heisenberg XYZ system. *Eur. Phys. J. D* **62**, 439–447 (2011)
15. Hu, M.L., Lian, H.L.: State transfer in intrinsic decoherence spin channels. *Eur. Phys. J. D* **55**, 711–721 (2009)
16. Yu, P.F., Cai, J.G., Liu, J.M., Shen, G.T.: Effects of phase decoherence on the entanglement of a two-qubit anisotropic Heisenberg XYZ chain with an in-plane magnetic field. *Eur. Phys. J. D* **44**, 151–158 (2007)
17. Guo, J.L., Song, H.S.: Effects of inhomogeneous magnetic field on entanglement and teleportation in a two-qubit Heisenberg XXZ chain with intrinsic decoherence. *Phys. Scripta* **78**, 045002 (2008)
18. Fan, K.M., Zhang, G.F.: Geometric quantum discord and entanglement between two atoms in Tavis–Cummings model with dipole–dipole interaction under intrinsic decoherence. *Eur. Phys. J. D* **68**, 163 (2014)
19. Shim, Yun-Pil, Oh, S., Hu, X.D., Friesen, M.: Controllable anisotropic exchange coupling between spin qubits in quantum dots. *Phys. Rev. Lett.* **106**, 180503 (2011)
20. Wootters, W.K.: Entanglement of formation of an arbitrary state of two qubits. *Phys. Rev. Lett.* **80**, 2245 (1998)
21. Hill, S., Wootters, W.K.: Entanglement of a pair of quantum bits. *Phys. Rev. Lett.* **78**, 5022 (1997)
22. Lee, J., Kim, M.S.: Entanglement teleportation via Werner states. *Phys. Rev. Lett.* **84**, 4236 (2000)
23. Jozsa, R.: Fidelity for mixed quantum states. *J. Mod. Opt.* **41**, 2315–2323 (1994)
24. Zhou, Y., Zhang, G.F.: Quantum teleportation via a two-qubit Heisenberg XXZ chain—effects of anisotropy and magnetic field. *Eur. Phys. J. D* **47**, 227–231 (2008)
25. Zhang, G.F.: Thermal entanglement and teleportation in a two-qubit Heisenberg chain with Dzyaloshinski–Moriya anisotropic antisymmetric interaction. *Phys. Rev. A* **75**, 034304 (2007)
26. Yeo, Y.: Studying the thermally entangled state of a three-qubit Heisenberg XX ring via quantum teleportation. *Phys. Rev. A* **68**, 022316 (2003)